

A global 86 GHz VLBI survey of compact radio sources

Sang-Sung Lee*

Max-Planck-Institut für Radioastronomie

E-mail: ssl@mpifr-bonn.mpg.de

Andrei P. Lobanov, Thomas P. Krichbaum, Arno Witzel, Anton Zensus

Max-Planck-Institut für Radioastronomie

E-mail: alobanov@mpifr-bonn.mpg.de, tkrichbaum@mpifr-bonn.mpg.de,

awitzel@mpifr-bonn.mpg.de, azensus@mpifr-bonn.mpg.de

Michael Bremer, Albert Greve, Michael Grewing

Institut de Radio Astronomie Millimétrique

E-mail: bremer@iram.fr, greve@iram.fr, grewing@iram.fr

We present results from a large global VLBI (Very Long Baseline Interferometry) survey of compact radio sources at 86 GHz which started in October 2001. The main goal of the survey is to increase the total number of objects accessible for future 3 mm-VLBI imaging by factors of 3 ~ 5. The survey data reach the baseline sensitivity of 0.1 Jy, and image sensitivity of better than 10 mJy/beam. To date, a total of 127 compact radio sources have been observed. The observations have yielded images for 109 sources, and only 6 sources have not been detected[†]. Flux densities and sizes of core and jet components of all detected sources have been measured using Gaussian model fitting. From these measurements, brightness temperatures have been estimated, taking into account resolution limits of the data. Here, we compare the brightness temperatures of the cores and secondary jet components with similar estimates obtained from surveys at longer wavelengths (e.g. 15 GHz). This approach can be used to study questions related to mechanisms of initial jet acceleration (accelerating or decelerating sub-pc jets?) and jet composition (electron-positron or electron-proton plasma?).

*The 8th European VLBI Network Symposium on New Developments in VLBI Science and Technology and EVN Users Meeting
September 26-29 2006
Torun, Poland*

*Speaker.

[†]The remaining 12 objects have been detected but could not be imaged due to insufficient closure phase information.

1. Observations

Millimeter wavelength VLBI (mm-VLBI) provides a unique tool for exploring the physical nature of compact radio sources. The higher resolution¹ of VLBI observations at millimeter wavelengths allows us to image directly the VLBI core and the knots with sub-pc scale resolution. Furthermore, in AGN synchrotron radiation becomes optically thin at wavelength between 1 cm and 1 mm [1]. Therefore, the mm-VLBI imaging makes it possible to look deeper into the VLBI cores, which are invisible at centimeter wavelengths. The first detection of single-baseline interference fringes of 89 GHz (3.4 mm) VLBI observation was reported by [2], demonstrating the feasibility of 3 mm VLBI. After a decade, the first global mm-VLBI array, the Coordinated Millimeter VLBI Array (CMVA), was established in 1995 with support from radio observatories throughout the world. The number of participating telescopes has gradually increased up to 12. The CMVA had stopped organizing mm-VLBI experiments in 2002. Since then, the activity of mm-VLBI experiments has been continued through the Global mm-VLBI Array (GMVA). The GMVA performs regular, coordinated global VLBI observations at 86 GHz, providing good quality images with a typical angular resolution of 50-70 micro-arcseconds (μ as). In order to increase the number of objects imaged at 86 GHz, four detection and imaging surveys have been conducted to date, with a total of 124 extragalactic radio sources observed at 86 GHz (see [3], [4], [5], [6]). Fringes have been detected in 44 objects, and so far only 24 radio sources have been successfully imaged. Table 1 gives us an overview of the VLBI surveys at 86 GHz. The survey presented here was envisaged as a project that would increase the number of objects imaged at 86 GHz by a factor of 3-5.

The source selection of this survey is based on the results from the VLBI surveys at 22 GHz [7], 15 GHz [8], and on source fluxes obtained from the multifrequency monitoring data from Metsähovi at 22, 37, and 86 GHz [9] and from Pico Veleta at 90, 150, and 230 GHz (Ungerechts, priv. comm.). Using these databases, we selected the sources with expected flux density above ≥ 0.3 Jy at 86 GHz. We excluded some of the brightest sources already imaged at 86 GHz, and focused on those sources which had not been detected or imaged in the previous surveys. Sources at higher northern declinations ($\delta > -40^\circ$) were preferred, in order to optimize the uv -coverage of the survey data. According to the afore-mentioned selection criteria, a total of 127 compact radio sources are selected and observed.

The survey observations have been conducted during three global mm-VLBI sessions on October 2001, April 2002 and October 2002. The participation of the large and sensitive European antennas (the 100-m radio telescope at Effelsberg, the 30-m mm-radio telescope at Pico Veleta, the 6 x 15-m interferometer on Plateau de Bure) results in a typical single baseline sensitivity of ~ 0.1 Jy and an image sensitivity of better than 10 mJy/beam. Every source in the survey was observed for 3-4 VLBI scans of 7-minutes duration (*snapshot* mode). The data were recorded either with a 128 MHz bandwidth or a 64 MHz bandwidth, using the MkIV VLBI system, with 1 and 2 bit sampling employed at different epochs. The observations were made in left circular polarization (LCP). We recorded 3-4 scans per hour, using the time between VLBI scans for antenna focusing, pointing and calibration. The data were correlated at the MkIV correlator in Max-Planck-Institut für Radioastronomie (MPIfR), Bonn. Fringes were searched with the HOPS package *fourfit* and

¹Global VLBI observations at 86 GHz offer a factor of 6 better resolution than space VLBI observations at 5 GHz.

Table 1: VLBI surveys at 86 GHz

Surveys	N_{ant}	ΔS	ΔI_{m}	D_{img}	N_{obs}	N_{det}	N_{img}
(1)	(2)	(3)	(4)	(5)	(6)	(7)	(8)
1	3	~ 0.5	45	12	...
2	2–5	~ 0.7	79	14	...
3	6–9	~ 0.5	~ 30	70	67	16	12
4	3–5	~ 0.4	~ 20	100	28	26	17
Total number of unique objects:					124	44	24
Properties of this survey:							
	12–14	~ 0.2	≤ 10	50	127	121	109

Notes: **Columns:** 1 - references of previous VLBI surveys at 86 GHz; 2 - number of participating antennae; 3 - average baseline sensitivity [Jy]; 4 - average image sensitivity [mJy/beam]; 5 - typical dynamic range of images; 6 - number of sources observed; 7 - number of objects detected; 8 - number of objects imaged. **References of surveys:** 1 - [3]; 2 - [4]; 3 - [5]; 4 - [6].

AIPS² task FRING. The amplitude calibration was performed using the system temperature, antenna gain, and opacity measurements performed at each station during the observations. The AIPS task APCAL is used to calibrate the amplitudes. From the phase- and amplitude-calibrated data, the images are made using DIFMAP software [10]. The detailed description for the fringe-fitting and imaging will be available in [11].

2. Images

We have detected 121 sources and produced hybrid maps of 109 sources for which the data contain a sufficiently large number of uv -points. Out of 109 sources, 90 sources are imaged for the first time at 86 GHz, increasing the number of sources ever imaged with 86 GHz VLBI observations up to 110. To illustrate our results, we present here images for two relatively weak objects. These are the first 3 mm-VLBI maps for the respective sources. For each image, plots of the uv -coverage and of the visibility amplitudes against uv -radius are presented. Here we report details on two sources.

0016+731:

The image in Figure 1 (top, right) shows two jet components along the different directions, $P.A. \sim -179^\circ$ and $P.A. \sim 150^\circ$, appearing to be bent to the southeast. The direction of the jet is in a good agreement with the VLBI images of 0016+731 obtained at 43 GHz [12] and 15 GHz [13]. The peak flux density is 0.196 Jy/beam with a beam size of 0.046×0.069 mas and the lowest contour level is 9.8 mJy. The brightness temperature (T_b) of the core component is $(2.5 \pm 0.8) \times 10^{11}$ K. Since the source is at high declination, the uv -sampling (shown in the left pannel) is nearly circular resulting in a very good restoring beam. The decrease of the visibility amplitude (middle panel) with the uv -distance (middle panel) indicates that the source is resolved.

²The NRAO Astronomical Image Processing System.

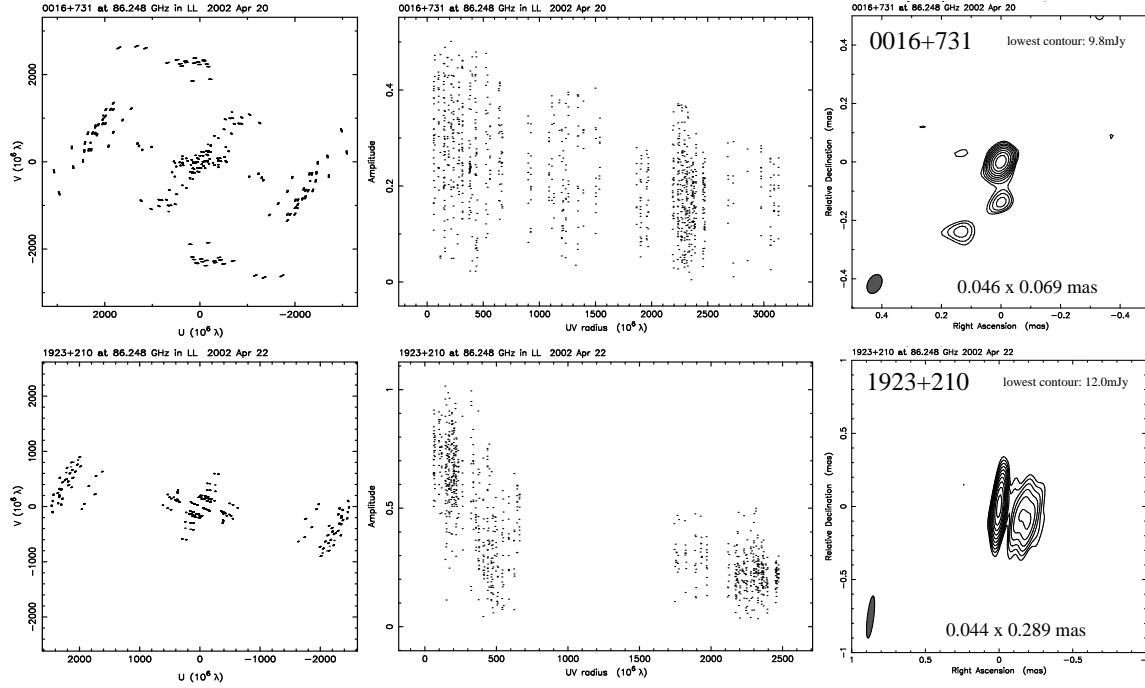


Figure 1: Images with the distribution of the uv -sampling and the visibility amplitudes of 0016+731 and 1923+210. The contours are drawn at $-1, 1, 1.4, \dots, 1.4^n$ of the lowest flux density levels, 9.8 mJy and 12.0 mJy, respectively.

1923+210:

In the image in Figure 1 (bottom, right), we identify one feature in the jet extending along $P.A. \sim -114^\circ$, which is similar to the orientation of the jet observed at lower frequencies[14]. The peak flux density is 0.301 Jy/beam, with a beam size of 0.044×0.289 mas, and the lowest contour level is 12.0 mJy. The brightness temperature of the core component is $(5.1 \pm 1.8) \times 10^{10} K$.

3. Brightness temperature and jet physics

Using the Gaussian-model fitted images of 109 sources, we have determined basic properties of the core and jet components for all of the imaged sources: total flux density, S_{tot} , peak flux density, S_{peak} , post-fit rms, σ_{rms} , size, d , radial distance, r (for jet componets), and position angle, θ (for jet componets). For all parameters, the uncertainties for measurements were obtained, taking into account the resolution limits [15]:

$$d_{\min} = \frac{2^{1+\beta/2}}{\pi} \left[\pi a b \ln 2 \ln \frac{SNR}{SNR-1} \right]^{1/2}, \quad (3.1)$$

which is the minimum resolvable size of a component in an image. The minimum resolvable size depends on the axes of the restoring beam, a and b , and the signal-to-noise ratio, SNR . The weighting function, β , is 0 for natural weighting or 2 for uniform-weighting. The observed brightness temperature, T_b , of a component in the rest frame of the source is given by

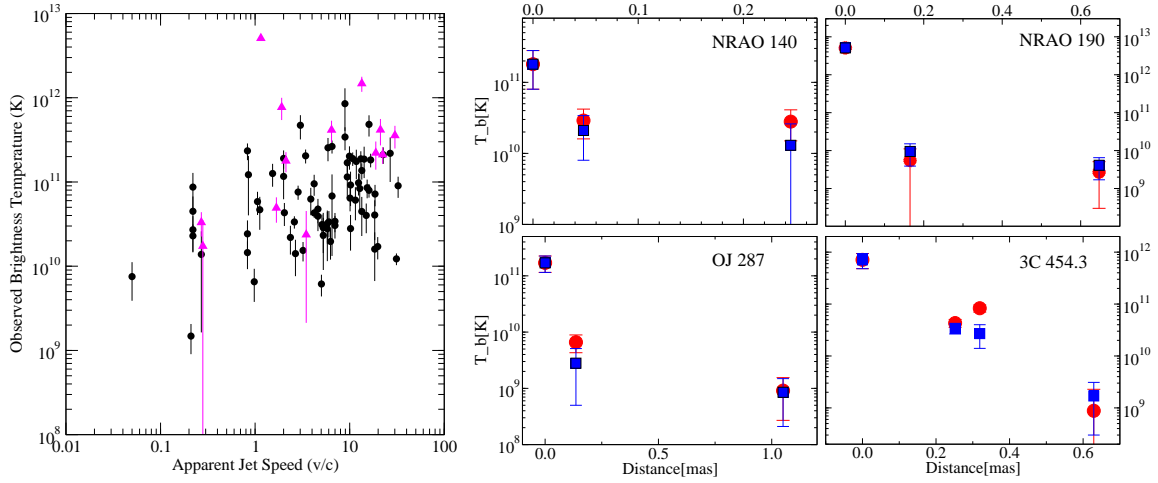


Figure 2: **Left:** A plot of measured T_b in the cores of the jets vs. maximum apparent jet speeds taken from 2 cm survey. Triangles are the lower limits. **Right:** Changes of the brightness temperature along the jets of several sources. Blue squares are the measured T_b . Red circles are the predicted T_b in adiabatically expanding shocks with the initial brightness temperature equal to that measured in the core of the jet.

$$T_b = \frac{2 \ln 2}{\pi k_B} \frac{S_{\text{tot}} \lambda^2 (1+z)}{d^2}, \quad (3.2)$$

where λ is the wavelength of observation, z is the redshift, and k_B is the Boltzmann constant. If $d < d_{\text{min}}$, then the lower limit of T_b is obtained with $d = d_{\text{min}}$. The observed brightness temperatures can be used to study the physics of the relativistic jets. One of the applications is to model the observed distribution of T_b by a population of jets in which all jets are randomly oriented and have the same Lorentz factor, γ_j , the same spectral index, α , and the same intrinsic brightness temperature, T_0 (see [6]). Since the orientation of the jets is random, and the observed distribution of T_b is caused only by Doppler boosting, the predicted distribution should be corrected for the bias due to the Doppler boosting. Lobanov et al. [6] applied this approach to a smaller sample of VLBI images at 86 GHz, inferring the range of $T_0 \sim 1 - 4 \times 10^{11} K$ that reproduces the observed distribution in the VLBI cores. We expect a similar result for our larger sample. Another application is to study the intrinsic brightness temperatures of the VLBI cores, by using the observed T_b at 86 GHz from our survey and the maximum apparent jet speeds at 15 GHz taken from [8]. The method from [16] could also be applied to our sample, in order to constrain the intrinsic brightness temperature. In the left panel of Figure 2, we can see a hint of correlation of the observed brightness temperatures of the VLBI cores with the maximum apparent jet speeds of the jets measured at 15 GHz. The right panel of Figure 2 shows the profile of T_b along the main jet direction. The predicted values of brightness temperatures in the jets by adiabatic expansion in a relativistic plasma [6] agree well with the observed brightness temperatures. Using these three approaches to analyzing the 86 GHz data, we hope to be able to further constrain physical models proposed to explain the nature of compact relativistic jets.

Acknowledgements

We gratefully thank the staff of the observatories participating in the GMVA; the MPIfR Effelsberg 100-m telescope, the two IRAM telescopes on Plateau de Bure and Pico Veleta, the Metsähovi Radio Observatory, the Onsala Space Observatory, and the VLBA. The VLBA is an instrument of the National Radio Astronomy Observatory, which is a facility of the National Science Foundation operated under cooperative agreement by Associated Universities, Inc.

References

- [1] J. A. Stevens, S. J. Litchfield, E. I. Robson, D. H. Hughes, W. K. Gear, H. Teräsranta, E. Valtaoja, and M. Tornikoski, *Multifrequency observations of blazars. 5: Long-term millimeter, submillimeter, and infrared monitoring*, *ApJ* **437** (1994) 91
- [2] A. C. S. Readhead, C. R. Mason, A. T. Moffet, et al., *Very long baseline interferometry at a wavelength of 3.4 mm*, *Nature* **303** (1983) 504
- [3] A. J. Beasley, V. Dhawan, S. Doeleman, and R. B. Phillips, *CMVA Observations of Compact AGNs, Proceedings of Millimeter-VLBI Science Workshop* (1997) 53
- [4] C. J. Lonsdale, S. S. Doeleman, and R. B. Phillips, *A 3 Millimeter VLBI Continuum Source Survey*, *AJ* **116** (1998) 8
- [5] F. T. Rantakyö, L. B. Baath, D. C. Backer, et al., *50 MU as resolution VLBI images of AGN's at lambda 3 MM*, *A&AS* **131** (1998) 451
- [6] A. P. Lobanov, T. P. Krichbaum, D. A. Graham, et al., *86 GHz VLBI survey of compact radio sources*, *A&A* **364** (2000) 391
- [7] G. A. Moellenbrock, K. Fujisawa, R. A. Preston, et al., *A 22 GHz VLBI Survey of 140 Compact Extragalactic Radio Sources*, *AJ* **111** (1996) 2174
- [8] K. I. Kellermann, R. C. Vermeulen, J. A. Zensus, and M. H. Cohen, *Sub-Milliarcsecond Imaging of Quasars and Active Galactic Nuclei*, *AJ* **115** (1998) 1295
- [9] H. Teräsranta, M. Tornikoski, A. Mujunen, et al., *Fifteen years monitoring of extragalactic radio sources at 22, 37 and 87 GHz*, *A&AS* **132** (1998) 305
- [10] M. C. Shepherd, T. J. Pearson, and G. B. Taylor, *Software Report: DIFMAP, Owens Valley Radio Observatory*, *BAAS* **26** (1994) 987
- [11] Sang-Sung Lee, *A Global 86 GHz VLBI Survey of Compact Radio Sources*, *PhD Thesis* at University of Bonn, in prep.
- [12] M. Lister, *Parsec-Scale Jet Polarization Properties of a Complete Sample of Active Galactic Nuclei at 43 GHz*, *ApJ* **562** (2001) 208.
- [13] M. Lister and D. C. Homan, *MOJAVE: Monitoring of Jets in Active Galactic Nuclei with VLBA Experiments. I. First-Epoch 15 GHz Linear Polarization Images*, *AJ* **130** (2005) 1389.
- [14] A. L. Fey and P. Charlot, *VLBA Observations of Radio Reference Frame Sources. III. Astrometric Suitability of an Additional 225 Sources*, *ApJS* **128** (2000) 17.
- [15] A. P. Lobanov, *Resolution limits in astronomical images*, *A&A*, submitted (astro-ph/0503225).
- [16] D. C. Homan, Y. Y. Kovalev, M. L. Lister, et al. *Intrinsic Brightness Temperatures of AGN Jets*, *ApJ*, **642** L115.